

# Roles of two successive phase transitions in new spin-Peierls system TiOBr

T. Sasaki,<sup>1</sup> M. Mizumaki,<sup>2</sup> T. Nagai,<sup>3</sup> T. Asaka,<sup>3</sup> K.

Kato,<sup>2,4</sup> M. Takata,<sup>2,4</sup> Y. Matsui,<sup>3</sup> and J. Akimitsu<sup>1</sup>

<sup>1</sup>*Department of physics, Aoyama-Gakuin University, Sagami-hara, Kanagawa 229-8558*

<sup>2</sup>*Japan Synchrotron Radiation Research Institute (JASRI), Spring-8, Hyogo 679-5198*

<sup>3</sup>*High Voltage Electron Microscopy Station,*

*National Institute for Materials Science, Tsukuba 305-0044*

<sup>4</sup>*CREST, Japan Science and Technology Corporation (JST), Kawaguchi, Saitama 332-0012*

(Dated: October 10, 2018)

## Abstract

In this study, we determine the roles of two successive phase transitions in the new spin-Peierls system TiOBr by electron and synchrotron X-ray diffraction analyses. Results show an incommensurate superstructure along the  $h$ - and  $k$ -directions between  $T_{c1}=27\text{K}$  and  $T_{c2}=47\text{K}$ , and a twofold superstructure which is related to a spin-Peierls lattice distortion below  $T_{c1}$ . The diffuse scattering observed above  $T_{c2}$  indicates that a structural correlation develops at a high temperature. We conclude that  $T_{c2}$  is a second-order lock-in temperature, which is related to the spin-Peierls lattice distortion with the incommensurate structure, and that  $T_{c1}$  is from incommensurate to commensurate phase transition temperature accompanying the first-order spin-Peierls lattice distortion.

PACS numbers: Valid PACS appear here

Low-dimensional  $S=1/2$  quantum spin systems have several unique features due to large quantum spin fluctuations. For instance, a one-dimensional (1D) chain coupled to three-dimensional lattice system undergoes spin-Peierls transition to a nonmagnetic dimerized state. This exotic phenomenon might be able to help us understand the roles of lattice and spin degrees of freedom in quasi-low-dimensional spin systems. Actually, detailed studies of the first inorganic spin-Peierls compound  $\text{CuGeO}_3$  have deepened the understanding of a spin-Peierls system, and opened higher level physics [1, 2].

Recently, Seidel *et al.* have suggested that  $\text{TiOX}$  ( $X=\text{Cl}, \text{Br}$ ) is a spin-Peierls compound with on orbital degree of freedom [3].  $\text{TiOX}$  has a  $\text{FeOCl}$ -type crystal structure [4, 5], where the  $\text{TiO}_4\text{X}_2$  bilayers separate from each other along the  $c$ -axis. The chains are composed of edge-shared  $\text{TiO}_4\text{X}_2$  octahedra in a direct contact with each other along the  $b$ -axis due to the occupation of the  $d_{xy}$  orbital in the ground state [3, 6]. It is still an open question whether the single valence of  $\text{Ti}^{3+}$  has occupied its orbital degree of freedom in this system [6, 7]. The evidence indicating that  $\text{TiOX}$  belongs to a new spin-Peierls system has been confirmed by the susceptibility [3, 8], nuclear magnetic resonance (NMR) [9, 14] and X-ray diffraction [5, 10, 11] measurements.

$\text{TiOBr}$  exhibits two successive phase transitions with  $T_{c1}=27\text{K}$  and  $T_{c2}=47\text{K}$ . The temperature dependence of susceptibility starts to gradually decrease at  $T_{c2}$  and show a sudden drop to zero at  $T_{c1}$ . These transitions have been reported to be of the first-order at  $T_{c1}$  and second-order transition at  $T_{c2}$  by NMR [14] and heat capacity measurements [15]. To elucidate the origin of these transitions, we have performed electron and synchrotron radiation (SR) X-ray diffraction analyses. Below  $T_{c1}$ , superlattice reflections were observed at  $(h, k + 1/2, l)$  positions, which are related to the spin-Peierls lattice distortion [5, 10]. If  $T_{c1}$  is the spin-Peierls transition temperature,  $\text{TiOX}$  is a new spin-Peierls compound having the first-order phase transition. Although the origin of the two successive phase transitions has not yet been clarified, Imai and Chou [14] suggested that "the emergence of the spin gap at  $T_{c2}$  is accompanied by an orbital-order (possibly incommensurate)". Above  $T_{c1}$ , we found the incommensurate superlattice reflections by SR X-ray and electron diffraction analyses [12]. Recently, these results have independently been confirmed by other research groups [7, 13]. In this paper, we discuss the key roles of two successive phase transitions.

Polycrystalline and single crystal of  $\text{TiOBr}$  samples were prepared by a chemical vapor transport technique [5, 8]. SR X-ray diffraction experiments were carried out using a four-

circle diffractometer at BL46XU, SPring-8. The X-ray wavelength determined using Si (111) monochromators was  $1.0332\text{\AA}$ . A single crystal with dimensions of  $1.5 \times 6 \times 0.03\text{mm}^3$  was glued on a BN plate, which was mounted on a refrigerator with the  $(hk0)$  reciprocal plane perpendicular to the  $\chi$ -axis. At electron diffraction analysis, a single crystal was thinned by  $\text{Ar}^+$  ion sputtering, and using a Hitachi HF-3000S high-voltage TEM operating at 300kV at the High Voltage Electron Microscopy Station, NIMS.

We examined the electron diffraction patterns at the  $(hk0)$  reciprocal lattice plane at various temperatures in the single crystal of  $\text{TiOBr}$ . Figure 1 shows the electron diffraction patterns of  $\text{TiOBr}$  at the  $(hk0)$  plane. At the  $(hk0)$  plane, where  $h$  and  $k$  are integers, strong reflections are indexed as fundamental reflections of orthorhombic  $Pmmn$ . However, weak spots are observed at  $h + k = 2n + 1$ , which are the forbidden reflections of orthorhombic  $Pmmn$ . The crystal symmetry of  $\text{TiOBr}$  may be different from that of orthorhombic  $Pmmn$ , because the forbidden reflections are observed even at room temperature [16]. Below  $T_{c1}$  (commensurate phase), the electron diffraction patterns show twofold superstructure along the  $k$ -direction at  $(h, k + 1/2, 0)$ , which is in good agreement with the X-ray diffraction results [5, 10]. The superlattice reflections split into two spots along the  $h$ -direction with diffuse scattering and are out of  $k = 1/2 + n$  along the  $k$ -direction (see Fig.1 (b) and (d)~(i)) above  $T_{c1}$ . To confirm the electron diffraction results, we performed an SR single crystal X-ray diffraction analysis. As shown in Fig.2, the twofold superstructure is observed below  $T_{c1}$ , and an incommensurate structure is produced along the  $h$ - and  $k$ -directions between  $T_{c1}$  and  $T_{c2}$  (intermediate region).

Figure 3 shows the temperature dependences of superlattice reflections around  $(0\ 2.5\ 0)$  determined by electron (open circle) and SR X-ray (closed circle) diffraction analyses. The electron diffraction result does not agree well with the X-ray diffraction result in the intermediate region. This is ascribed to the difference in sensitivity to atoms between the electron and X-ray probes. In addition, as the sample is locally heated by the electron diffraction technique, temperature is unstable around the observed area. Therefore, it is difficult to observe clearly separated incommensurate double peaks along the  $h$ -direction in electron diffraction, although the clear incommensurate peaks are observed in SR X-ray diffraction (compare Fig.1 and Fig.2). The remarkable behaviors of  $\delta_h$  and  $\delta_k$  at  $T_{c1}$  and  $T_{c2}$  are shown in Fig.3;  $\delta_h$  continuously changes only within the intermediate region and becomes constant ( $0.083[\text{r.l.u.}]$ ) above  $T_{c2}$ .  $\delta_k$  jumps from 0.5 to 0.495 at  $T_{c1}$  with increasing

temperature, and is inversely proportional to temperature above  $T_{c1}$ , which is expressed as the function  $\delta_k \propto -4.5 \times 10^{-4}T$ . The jumps of  $\delta_h$  and  $\delta_k$  at  $T_{c1}$  imply a first-order incommensurate (above  $T_{c1}$ ) to commensurate (below  $T_{c1}$ ) phase transition. However,  $\delta_k$  is unaffected by the phase transition at  $T_{c2}$ ; in other words,  $\delta_h$  and  $\delta_k$  behave independently at  $T_{c2}$ . This result implies that each temperature has a unique essential role in spin-Peierls transition

Figure 4 shows the temperature dependences of the integrated intensities of superlattice reflections measured by  $\omega$ -scan at around (0 2.5 0). The two integrated intensities of the incommensurate reflections at  $(\pm\delta_h, 2 + \delta_k, 0)$  are similar in this experiment [17], and gradually decrease to  $T_{c2}$ . This implies that  $T_{c2}$  is a second order phase transition temperature. The dashed line in Fig.4 is a fitting result within the intermediate region at  $(-\delta_h, 2 + \delta_k, 0)$  obtained using the function  $I_{inco}(T) \propto (1 - T/T_{c2})^{2\beta}$  with  $T_{c2} = 47.0 \pm 0.1\text{K}$  and  $2\beta = 0.193 \pm 0.071$  [18].  $\beta$  is the exponent obtained from the temperature dependence of the atomic displacement  $d$  since  $I \propto d^2$ . The fitting result demonstrates that  $\beta$  of TiOBr does not agree with the value ( $2\beta = 0.66$ ) of CuGeO<sub>3</sub>. The integrated intensities tend to decrease at around  $T_{c1}$ . This is probably due to the fact that we could not measure the intensities accurately because the superlattice reflections are always accompanied by the diffuse scattering along the  $h$ -direction in the vicinity of  $T_{c1}$  (see Fig.2 at 25K).

To measure the critical fluctuations at  $T_{c1}$  and  $T_{c2}$ , we chose the strongest superlattice peak at  $(-2 + \delta_h, 3 + \delta_k, 1)$ . The correlation lengths,  $\xi$ , of the critical fluctuations were determined from the reciprocal of half width at half maximum, HWHM, which was corrected on the basis of the experimental resolution. Figure 5 shows the temperature dependences of HWHM along the  $h$ -,  $k$ - and  $l$ -directions. HWHM behaves as  $\sqrt{(T - T_{c2})}$  with the average value of  $T_{c2} = 48.7 \pm 1.5\text{K}$ . The diffuse scattering along the  $h$ - and  $l$ -directions seems to be wider than that along the  $k$ -direction at  $T_{c1}$  and above  $T_{c2}$ .  $\xi_k$  decreases very slowly with increasing temperature, such as  $\xi_k = 272\text{\AA}$  ( $= 78 \times b$ ) at 51K. The anisotropy ratio of correlation lengths at 51K is  $\xi_h : \xi_k : \xi_l \sim 1.5 : 13 : 1$ . This implies that the correlation length along chains increases at a high temperature (for example,  $\xi_k < b = 13158\text{K}$ ) in this system.

Our present study unambiguously shows that the superlattice reflections split along the  $h$ - and  $k$ -directions from the twofold superstructures along the  $h$ -direction at  $(h, k + 1/2, 0)$  above  $T_{c1}$ . The incommensurate structures along the  $h$ - and  $k$ -directions behave of each

other independently. We believe that clarifying the origin of incommensurate structure is the key to understanding the TiOX system.

Recently, Rückamp *et al.* and van Smaalen *et al.* have suggested the crystal structure in the incommensurate phase for TiOBr [7, 13]; however, they could not experimentally determine whether the final structure is monoclinic or orthorhombic (see Fig.3 of van Smaalen *et al.*), because they did not have the direct information on the crystal symmetry. Our electron diffraction result provides more information necessary for discussing for the crystal symmetry. The incommensurate peaks are different between Fig.1 (e) and (f), which implies that there are two domains perpendicular to the chain direction at the  $(hk0)$  plane, as confirmed by selected-area electron diffraction. More detailed experiments for crystal symmetry determination are now in progress [16]. In SR X-ray diffraction analysis, the integrated intensities of both the commensurate at  $(0\ 2.5\ 0)$  and the incommensurate (total) are scaled using the universal function (the solid line in Fig.4), which indicates that the relationship between the commensurate and incommensurate phases is not independent of roles. The integrated intensity of the superlattice reflection is directly related to the length of the lattice distortions, for which energy may be stored in the vicinity of  $T_{c1}$ .

The lattice distortion with the incommensurate structure occurs at  $T_{c2}$ . The twofold superlattice reflections confirm the presence of the (commensurate) spin-Peierls lattice distortion below  $T_{c1}$ , at which the first order incommensurate to commensurate phase transition occurs. Here, we indicate the phenomena occurring at  $T_{c1}$  and  $T_{c2}$ , and the roles of the two successive phase transition

As shown in Fig.3,  $\delta_k$  is not affected by the lattice distortion with the incommensurate structure at  $T_{c2}$ , and the anisotropic diffuse scattering is produced above  $T_{c2}$  up to 150K, which corresponds to the results of ESR and infrared optical properties [6, 19, 20]. With decreasing temperature down to  $T_{c2}$ , the structural short-ranged correlation length increases. Although the structural distortion becomes long-ranged at  $T_{c2}$ , no twofold distortion is observed in the intermediate region. Since the incommensurate superstructure along the  $k$ -direction is dominated by the strength of interchain interaction, the unaffected  $\delta_k$  at  $T_{c2}$  clearly shows that the interaction within chains is dominant in this material. As shown in Fig.5, the strong diffuse scattering above  $T_{c2}$  is observed, which clearly indicates the local lattice distortion due to the spin-Peierls instability.

As shown in Fig.3, the incommensurability along the h-direction,  $\delta_h$  ( $=0.083$ ), is almost

equal to the twelvefold unit cell, which approximately corresponds to the correlation length that relaxes the frustration between chains. The displacement of one atom strongly influences the neighboring atoms. Below 150K, the local incommensurate structure is caused by the short-ranged distortion within chains, and exhibits on interchain interactions with twelvefold correlation lengths. This is considered to be the key role of the diffuse scattering with the incommensurate structure. With decreasing temperature, the long-ranged distortion with the incommensurate structure is locked in at  $T_{c2}$ . Between  $T_{c1}$  and  $T_{c2}$ ,  $\delta_k$  increases toward  $1/2$ . This is because the intrachain interaction (commensurability energy) overcomes the interchain interaction (incommensurability energy), and the commensurability accompanying the first-order transition is established.

In summary, the incommensurate to commensurate phase transition was clearly observed by electron and SR x-ray diffraction analyses in the single crystal of TiOBr. Superlattice reflections were observed at  $(h, k + 1/2, l)$  below  $T_{c1}$  and at  $(h \pm \delta_h, k + \delta_k, l)$ ;  $h, k, l = \text{integer}$  and  $h + k = 2n$  for  $(hk0)$ , above  $T_{c1}$ . The diffuse scattering was clearly observed along the  $h$ - and  $l$ -directions at  $T_{c1}$  and above  $T_{c2}$ , indicating the development of the structural correlation along chains far above  $T_{c2}$ . This suggests that  $T_{c1}$  is a first-order incommensurate to commensurate phase transition temperature with the spin-Peierls lattice distortion, and that  $T_{c2}$  is a second order lock-in temperature, which is related to the spin-Peierls lattice distortion with the incommensurate structure

## Acknowledgments

We would like to thank H. Sawa and T. Yokoo (KEK) for having interest in this work and for fruitful discussion. The Aoyama-Gakuin group was partly supported by the 21<sup>st</sup> COE program. The synchrotron radiation experiment was performed at BL46XU (R04B46XU-0020N) in SPring-8 with the approval of the Japan Synchrotron Radiation Research Institute (JASRI). A part of the electron diffraction experiment was supported by the "Nanotechnology Support Project" of the Ministry of Education, Culture, Sports, Science and Technology, MEXT, Japan

---

[1] M. Hase, I. Terasaki and K. Uchinokura, Phys. Rev. Lett. **70**, 3651 (1993)

- [2] M. Hase, I. Terasaki, Y. Sasago, K. Uchinokura and H. Obara, Phys. Rev. Lett. **71**, 4059 (1993)
- [3] A. Seidel, C. A. Marianetti, F. C. Chou, G. Ceder and P. A. Lee, Phys. Rev. B **67**, 020405(R) (2003)
- [4] R. J. Beynon and J. A. Wilson, J. Phys.: Condens. Matter **5**, 1983 (1993)
- [5] T. Sasaki, M. Mizumaki, K. Kato, Y. Watabe, Y. Nishihata, M. Takata and J. Akimitsu, J. Phys. Soc. Jpn. **74**, 2185 (2005)
- [6] V. Kataev, J. Baier, A. Moller, L. Jongen, G. Meyer and A. Freimuth, Phys. Rev. B **68**, 140405(R) (2003)
- [7] R. Rückamp, J. Baier, M. Kriener, M. Haverkort, T. Lorenz, G. Uhrig, L. Jongen, A. Moller, G. Meyer and M. Gruninger, cond-mat/0503409 (2005)
- [8] C. Kato, Y. Kobayashi and M. Sato, J. Phys. Soc. Jpn **74**, 473 (2005)
- [9] J. Kikuchi *et al.* (private communication)
- [10] M. Shaz, S. van Smaalen, L. Palatinus, M. Hoinkis, M. Klemm, S. Horn and R. Claessen, Phys. Rev. B **71**, 100405(R) (2005)
- [11] L. Palatinus, A. Schonleber and S. van Smaalen, Acta Crystallogr., Sect. C: Crystallogr. Struct. Commun. **61**, i48 (2005)
- [12] T. Sasaki, M. Mizumaki, T. Nagai, T. Asaka, K. Kato, M. Takata, Y. Matsui and J. Akimitsu, to be published in Physica B
- [13] S. van Smaalen, L. Palatinus and A. Schonleber, Phys. Rev. B **72**, 020105(R) (2005)
- [14] T. Imai and F. C. Chou, cond-mat/0301425 (2003)
- [15] J. Hemberger, M. Hoinkis, M. Klemm, M. Sing, R. Claessen, S. Horn and A. Loidl, cond-mat/0501517 (2005)
- [16] T. Sasaki, T. Nagai, K. Kato, M. Mizumaki, T. Asaka, Y. Matsui M. Takata and J. Akimitsu: unpublished
- [17] We attempt to measure the integrated intensity of each incommensurate reflection several times. Actually, the values at  $(\pm\delta_h, 2+\delta_k, 0)$  indicate the difference in intensity, although each intensity indicates the same behavior with decreasing temperature. Because the incommensurate structure has two domains, the intensity represents the ratio of the domains illuminated by the probes.
- [18] The data from 40-48 K is fitted with  $T_{c2} = 47.8 \pm 1.0\text{K}$  and  $2\beta = 0.513 \pm 0.186$ , although

Figure 4 does not show the line.

- [19] G. Caimi, L. Degiorgi, N. N. Kovaleva, P. Lemmens and F. C. Chou, Phys. Rev. B **69**, 125108 (2004)
- [20] P. Lemmens, K. Y. Choi, G. Caimi, L. Degiorgi, N. N. Kovaleva, A. Seidel and F. C. Chou, Phys. Rev. B **70**, 134429 (2004)



## Figure captions

Figure 1 Electron diffraction patterns of TiOBr at  $(hk0)$  plane. (a) Commensurate phase, (b) incommensurate (intermediate) phase, (c) high-temperature phase, and (d)~(i) temperature dependence of superlattice reflections around  $(040)$ .

Figure 2 SR X-ray diffraction mesh scans around  $(0\ 2.5\ 0)$  on  $(hk0)$  plane at each temperature. Intensities are normalized using monitor counts and shown on the log scale.

Figure 3 Temperature dependences of (a)  $\delta_h$  and (b)  $\delta_k$  at  $(-\delta_h, 2 + \delta_k, 0)$  determined by electron (open circle) and SR X-ray (closed circle) diffractions analyses.

Figure 4 Temperature dependences of integrated intensities of superlattice reflections measured by  $\omega$ -scan around  $(0\ 2.5\ 0)$ . We measured the reflections at two incommensurate positions  $(-\delta_h, 2 + \delta_k, 0)$  (open square) and  $(\delta_h, 2 + \delta_k, 0)$  (closed triangle) above  $T_{c1}$ , and at a commensurate position  $(0\ 2.5\ 0)$  (open circle) below  $T_{c1}$ . Closed circles indicate the total intensities of the two incommensurate intensities. The inset shows the rocking curves obtained at  $(0\ 2.5\ 0)$  7.5K (closed square),  $(0.0773, 0.4897, 0)$  32.5K (open triangle) and  $(0.083, 0.4838, 0)$  49K (cross).

Figure 5 Temperature dependences of HWHM of superlattice peaks at  $(-2 - \delta_h, 3 + \delta_k, 1)$  along  $h$ -(open circle),  $k$ -(closed square) and  $l$ -(closed triangle) directions. The lines indicate the best fits of these data to a  $\sqrt{(T - T_{c2})}$  law. The inset shows the diffuse scatterings at 45K (closed circle), 50K (open square) and 57.5K (cross) along the  $h$ -direction.

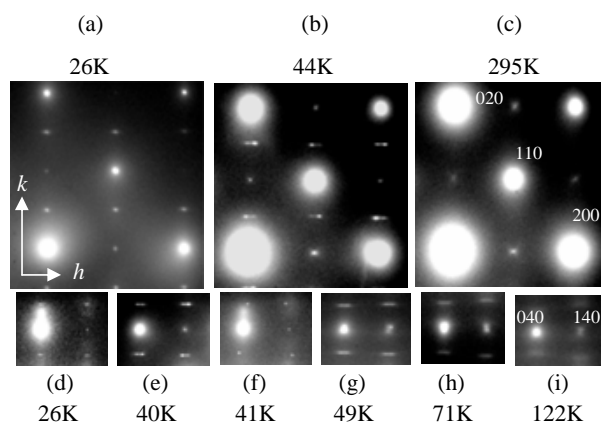


FIG. 1:

Fig.1 T. Sasaki *et al.*

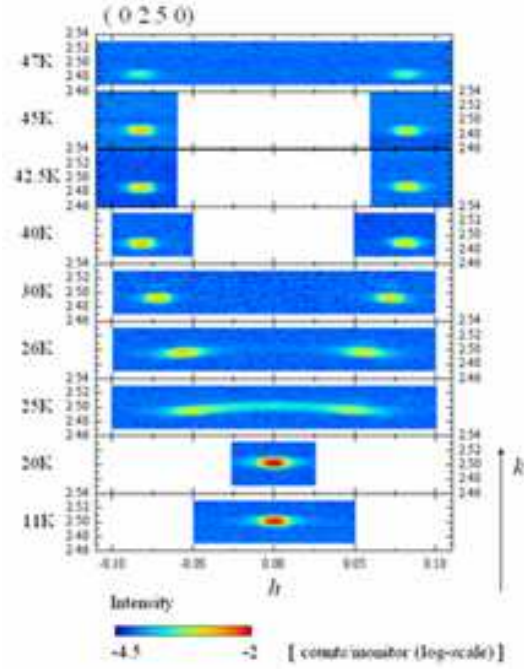


FIG. 2:

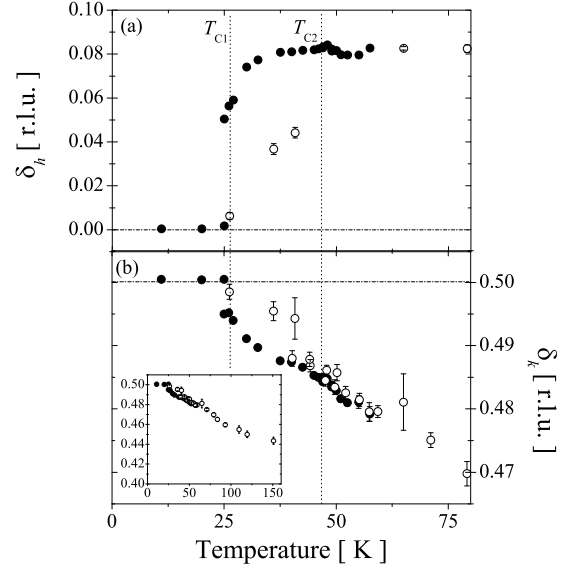


FIG. 3:

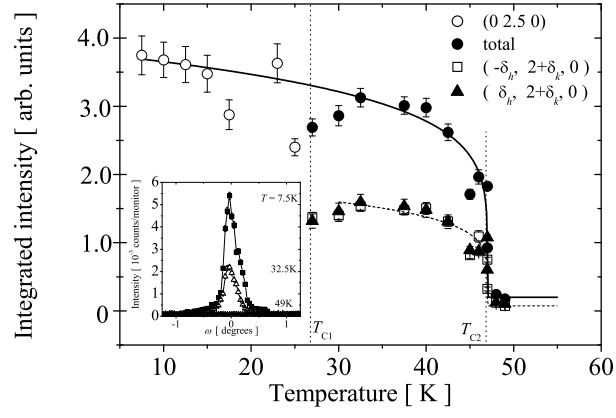


FIG. 4:

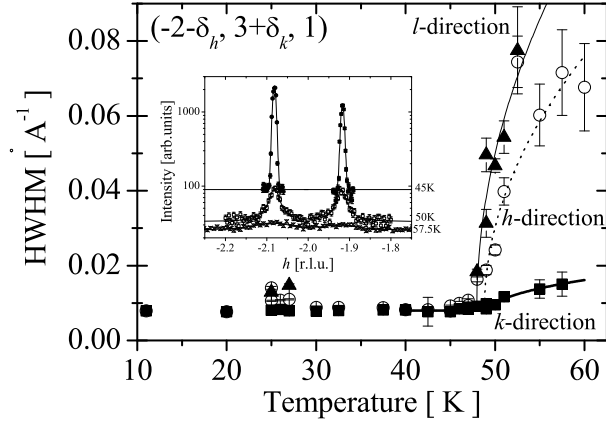


FIG. 5: